Department of Pharmacy[1], Faculty of Pharmacy, Mahidol University, Bangkok, Department of Pharmaceutical Technology[2], Faculty of Pharmaceutical Sciences, Prince of Songkla University, Songkhla, Thailand, School of Pharmacy[3], University of Otago, Dunedin, New Zealand

Characterisation of microstructures formed in isopropyl palmitate/water/Aerosol®OT : 1-butanol (2 : 1) system

P. Boonme[1,2], K. Krauel[3], A. Graf[3], T. Rades[3], V. B. Junyaprasert[1]

Received January 31, 2006, accepted March 5, 2006

Assoc. Prof. Dr. V. B. Junyaprasert, Department of Pharmacy, Faculty of Pharmacy, Mahidol University, Bangkok 10400, Thailand
pyvbp@mahidol.ac.th

Pharmazie 61: 927–932 (2006)

The aim of this work was to determine the type and microstructure of microemulsion samples formed in IPP/water/Aerosol®OT : 1-butanol (2 : 1) systems as a case study for the investigation of microemulsions. The concentration of the surfactant/cosurfactant mixture was kept constant while the ratio of water to oil was varied. Several techniques were used to investigate the types and phase transitions of the microemulsion formulations. The experimental methods used included visual observation cross-polarized light microscopy (PLM) appearance, conductivity, viscosity, cryo-field emission scanning electron microscopy (cryo-FESEM), differential scanning calorimetry (DSC), nuclear magnetic resonance (NMR), and fluorescence resonance energy transfer (FRET). Taken together, the results of the various techniques imply that the systems investigated are undergoing two transitions as a function of water concentration. Between 10–15%w/w of water, the systems change from headgroup hydrated surfactant solutions in oil (or possibly very small reversed micellar systems) to w/o microemulsions. These systems then change to o/w microemulsions between 25–30%w/w of water. The transitions however, appear to be gradual, as for example the DSC data indicates a transition between 15–20%w/w of water. Furthermore, for some methods the changes observed were very weak, and only with supportive data of other techniques can the phase behaviour of the microemulsion systems be interpreted with confidence. Interestingly, no indication of the presence of a bicontinuous intermediate microstructure was found. Liquid crystal formation was detected in samples containing 55%w/w of water.

1. Introduction

Microemulsions are optically transparent, low viscous and thermodynamically stable dispersions of oil and water stabilized by an interfacial film of a surfactant, usually in combination with a cosurfactant. In pharmaceutics, microemulsions are used as vehicles for drug delivery *inter alia* because of their good appearance, stability and ease of preparation. Microemulsions can be separated into three types: water-in-oil (w/o), bicontinuous and oil-in-water (o/w) (Paul and Moulik 1997; Lawrence and Rees 2000). Aerosol®OT has been frequently used as a surfactant in pharmaceutical microemulsion formulation (Changez and Varshney 2000; El-Laithy 2003; Gupta et al. 2005; Mitra and Paul 2005) and thus was also used as a surfactant in this study. Understanding the relationship between microstructure and composition of microemulsions is important if one wants to prepare these colloidal formulations efficiently for use in pharmaceutical applications; however, the characterisation of microemulsions is complex and usually requires the combination of several techniques.

Experimental techniques that have been used to characterise microemulsion structures include conductivity, viscosity, differential scanning calorimetry (DSC), small-angle X-ray scattering (SAXS), nuclear magnetic resonance (NMR), freeze-fracture transmission electron microscopy (FF-TEM) and cryo-field emission scanning electron microscopy (cryo-FESEM) (Moulik and Paul 1998; Garti et al. 2000; Alany et al. 2001; Ko et al. 2003; Bumajdad and Eastoe 2004; Moshe et al. 2004; Podlogar et al. 2004; Krauel et al. 2005; Mitra and Paul 2005). Each technique provides different information and can be used to support the results of other techniques to investigate the type and microstructure of microemulsions. In this study, fluorescence resonance energy transfer (FRET) was also used to study the microstructure of microemulsions. FRET is a distance-dependent interaction between electrons in the exited state of two dye molecules in which excitation is transferred from a donor molecule to an acceptor molecule without emission of a photon. FRET has been demonstrated to be a useful technique in the investigation of topographical information of proteins, nucleic acids and biological membrane systems (Selvin 2000; Takenaka et al. 2003; Lovullo et al. 2005). It can also be used for detecting changes in the distance between fluorophores which are dissolved in an aqueous phase; therefore, it might be

useful for the detection of changes in the state of water in microemulsion systems with increasing water concentrations. To our knowledge, no report to date has dealt with the use of FRET to study microemulsion systems.

The aim of this work was to determine the type and microstructure of microemulsion samples formed in IPP/water/Aerosol®OT : 1-butanol (2 : 1) systems as a case study for the investigation of microemulsions. The concentration of the surfactant/cosurfactant mixture was kept constant while the ratio of water to oil was varied. Several techniques were used to investigate the types and phase transitions of the microemulsion formulations.

2. Investigations and results

2.1. Phase diagram and appearance of samples

Fig. 1 shows the pseudoternary phase diagram of the IPP/water/Aerosol®OT : 1-butanol (2 : 1) system where the area inside the frame assigned on the phase diagram was the microemulsion region. The area outside the frame indicates multiphase turbid regions. It was noted that the area of the microemulsion region was fairly large since 1-butanol acted as a cosurfactant and interacted with the surfactant monolayer to increase the flexibility of the interfacial film (Alany et al. 2000).

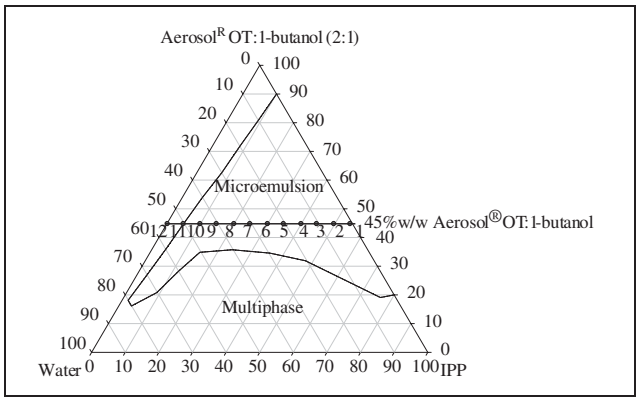

Fig. 1: Pseudoternary phase diagram of IPP/water/Aerosol®OT : 1-butanol (2 : 1) system at room temperature (25 °C). Samples selected for further investigation are numbered 1–12

Samples 1–11 were clear colorless liquids and isotropic when investigated by cross-polarized light microscopy; hence, they were designated as microemulsions (or in case of sample 1 as a reversed micellar solution due to the absence of water). Sample 12 was a gel-like product and birefringence was found under the cross-polarized light microscope. This sample was designated as a liquid crystalline sample. One of the easiest ways to distinguish liquid crystals and microemulsions is their observation under the cross-polarized light microscope. Birefringence is found in most lyotropic liquid crystals (exception: cubic phases) but is not found in microemulsions (Friberg 1990). The textures found in the cross-polarized light microscope identified the liquid crystal as lamellar (maltese crosses, oily streaks, data not shown).

2.2. Cryo-FESEM

Cryo-FESEM micrographs of some representative samples formed along the sampling path marked by the line on the pseudoternary diagram are shown in Fig. 2. No discernable fine structure could be visualized in samples containing less than 10%w/w of water (samples 1–3). If reversed micelles have formed at a low water concentration, their size was too small to be detected. Globular structures were found when the water concentrations were higher than 10%w/w (samples 4–11). Thus, when the water concentration was increased, the micrographs implied that droplet microemulsions were formed. In none of the samples structures resembling a bicontinuous microemulsion were found (Alany et al. 2001; Krauel et al. 2005).

2.3. Conductivity

Fig. 3 shows the relationship between water concentration and conductivity of the samples. In this work the conductivity measurements were carried out without incorporation of electrolyte to avoid phase changes due to the addition of salt (Podlogar et al. 2004). The conductivity of the studied samples was very low as long as the water fraction was smaller than 10%w/w (sample 3). At higher water concentrations an increase in conductivity was observed. A further, albeit only slight, change in the conduc-

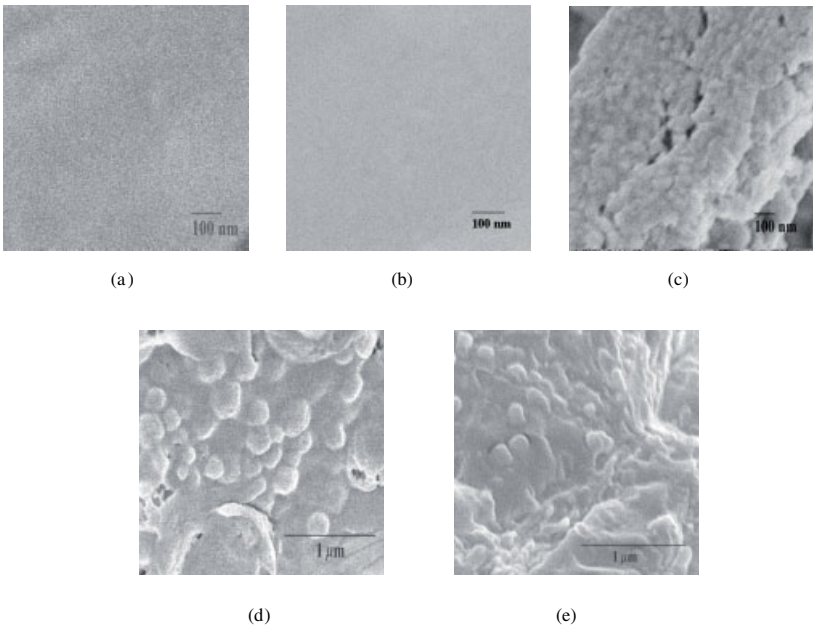

Fig. 2:
Cryo-FESEM micrographs of (a) sample 1 (0%w/w of water), (b) sample 3 (10%w/w of water), (c) sample 4 (15%w/w of water), (d) sample 7 (30%w/w of water) and (e) sample 9 (40%w/w of water). Magnification is indicated on each micrograph

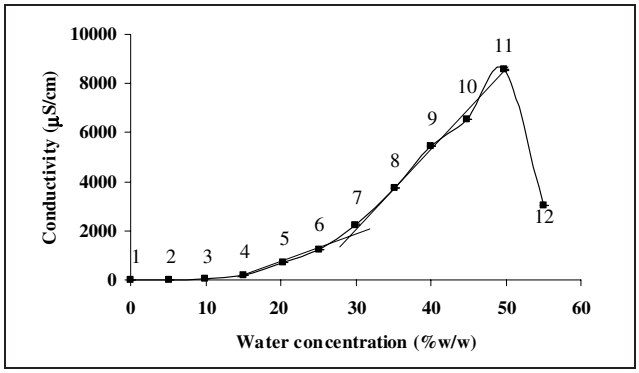

Fig. 3: Conductivity as a function of water concentration of samples 1–12 at 25 °C

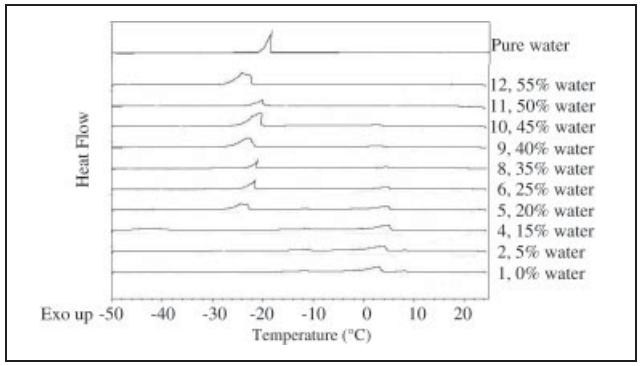

Fig. 5: DSC cooling curves as a function of water concentration of samples 1–2, 4–6, 8–12 and pure water

tivity plot could be observed upon addition of 30%w/w of water (sample 7). Increase in the water concentration of over 50%w/w (sample 12) led to a drastic decrease in the conductivity values coinciding with the formation of a liquid crystalline sample.

2.4. Viscosity

Viscosity of all samples remained almost constant until 50%w/w water concentration (sample 11) and then increased sharply because of liquid crystal formation (Fig. 4). All samples, except for sample 12, showed Newtonian flow, typical of microemulsions (Alany et al. 2001). The viscosity values of samples with 0 to 50%w/w of water (samples 1–11) were low and relatively constant at 5 to 8 mPas. There was a small change in viscosity between a water concentration of 15 and 30%w/w (samples 3–5, Fig. 4, inset); however, the changes were deemed too small to allow a structural interpretation.

2.5. Differential scanning calorimetry (DSC)

When water is present in a microemulsion system, it can be either bound or free water depending on the state of the system. Therefore, the exothermic freezing peak of water in the thermograms of each sample was compared with that of pure water to detect changes in the state of water, and thus changes in the microstructure of the microemulsion (Fig. 5).

Upon cooling pure water in the DSC a large exotherm with a peak onset of −18 °C was found (freezing of water). At low water fractions (<20%w/w, samples 1–4), a freezing peak for water could not be detected. When the water fractions were increased (≥20%w/w, samples 5–11), a freezing exotherm close to but always lower than −18 °C was found. The freezing point of water increased in samples 5–11 from approximately −23 to −20 °C.

Bulk (free) water is assumed to have physicochemical properties similar to those of pure water. Bound water on the other hand is strongly influenced by the surfactants present in the samples and its properties will differ from those of pure water, i.e. the presence of a nearby surfactant alters its thermodynamic properties such as freezing point, melting point, enthalpy and heat capacity (Garti et al. 2000; Podlogar et al. 2004). A freezing peak of water in IPP/water/Aerosol®OT : 1-butanol (2 : 1) could be observed in samples containing more than 20%w/w of water, indication that water might change its state from "internal" to "external" at this point.

The freezing point in sample 12, containing of 55%w/w of water, was again shifted to a lower temperature (−23 °C). This shift of the freezing point is likely to be caused by the formation of a liquid crystalline phase. It should be noted that no samples showed a freezing peak at the same position as pure water (−18 °C), indicating that in the studied microemulsions interactions between surfactant mixture and water were always present, albeit to different degrees.

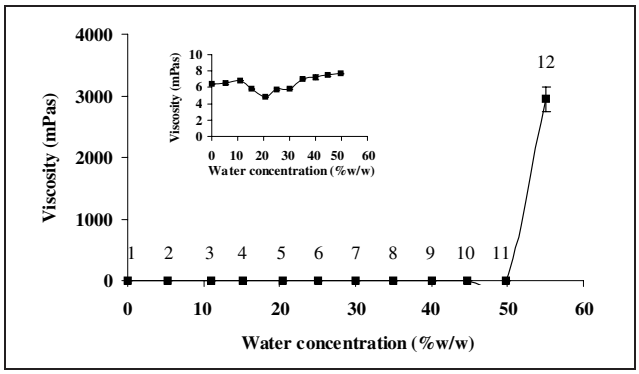

Fig. 4: Viscosity as a function of water concentration of samples 1–12 at 25 °C

2.6. Self-diffusion NMR

The positions of characteristic NMR peaks for water and IPP are shown in Fig. 6 at around 4.6 and 2.4 ppm, respectively. The self-diffusion coefficients of water and IPP in the studied systems were calculated. By comparing the self-diffusion coefficients of water and IPP in the microemulsion samples with those of the single components, the microemulsion type can be determined (Stilbs 1987; Kreilgaard et al. 2000; Ko et al. 2003; Krauel et al. 2005).

If the microemulsion system is of a droplet-type, the self-diffusion of the components of the internal pseudo-phase is determined by the diffusion of the droplet itself and therefore will be slow. In a bicontinuous microemulsion, where both oil and water are forming larger domains, the diffusion of both components is high and of the same magnitude as that observed for the pure components (Stilbs 1987; Kreilgaard et al. 2000). The self-diffusion coefficients of pure IPP and pure water were 1.58×10^{-11} and 7.98×10^{-11} m/s^2, respectively. The self-diffusion coefficients of IPP and water in samples 1–11 are presented in Fig. 7 and lower than that of the pure components. At water concentrations of 5 and 10%w/w, the self-diffusion coefficient of water initially stays constant (samples 2–3), but increases at water concentrations of 15%w/w

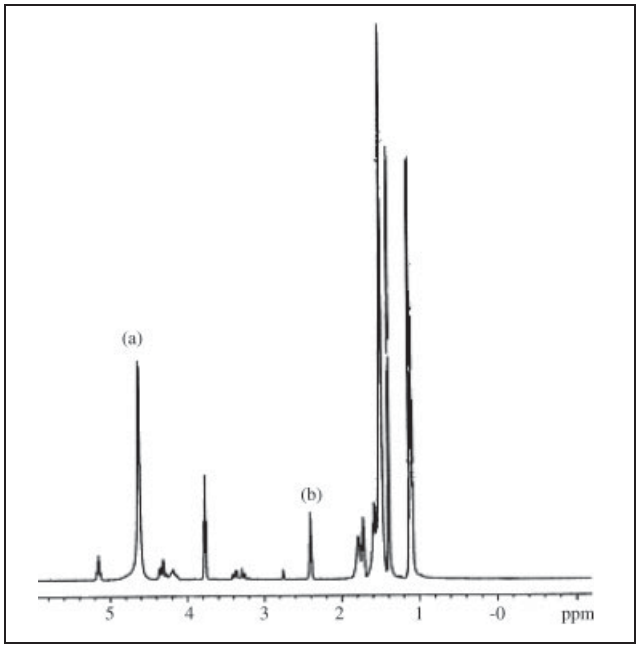

Fig. 6: ^{1}H NMR spectra of a sample 4. The symbols (a) and (b), indicate characteristic peaks for water and IPP, respectively

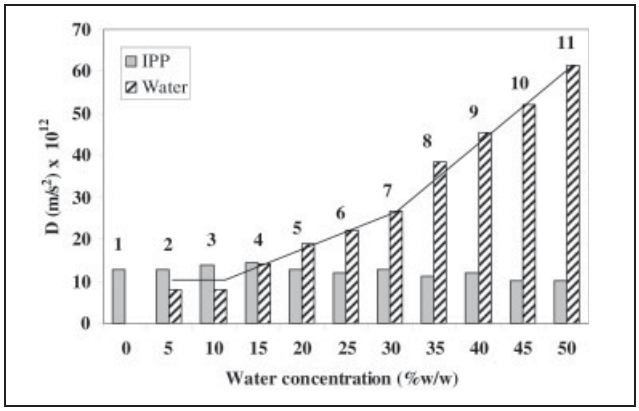

Fig. 7: The self-diffusion coefficients of IPP and water in IPP/water/Aerosol®OT: 1-butanol (2 : 1) systems containing various concentrations of water from 0 to 50% (w/w) (samples 1–11)

and higher (samples 4–11). Between samples 7–8 (30–35%w/w of water, respectively) a strong increase in the water self-diffusion coefficient was found.

The self-diffusion coefficient of water was higher than that of IPP from a water concentration of 20%w/w (sample 5) onwards. Sample 5 was also the first sample to show a decreased self-diffusion for IPP. The self-diffusion coefficient of IPP further decreased upon increase of water concentration (samples 5–11).

2.7. Fluorescence resonance energy transfer (FRET)

The 5(6)-FAM solution has a maximum emission at a wavelength of 515 nm, whereas 5(6)-TEMRA solution has a maximum emission at 570 nm when they were excited by light of a wavelength of 488 nm. It was found in the emission spectra of the microemulsion samples containing the dye mixture solution as aqueous phase, that the intensity of 5(6)-FAM emission peak decreased while the intensity of 5(6)-TEMRA emission peak increased when compared with the intensities of emission peaks of the pure dyes

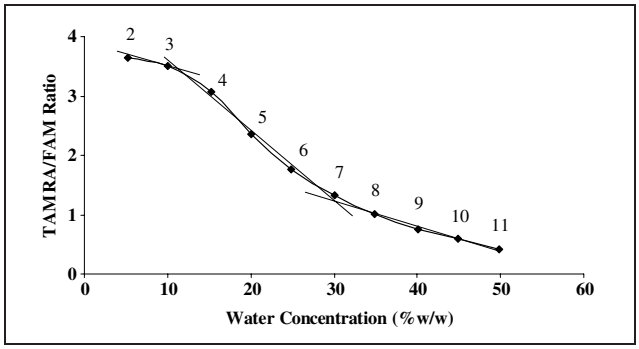

Fig. 8: The TAMRA/FAM ratios of the samples as a function of water concentration at 25 °C

dissolved in water at the same concentration, indicating that 5(6)-FAM transferred energy to 5(6)-TEMRA, i.e. a certain degree of FRET took place between the dyes.

It can be seen in Fig. 8 that the intensity ratios of the emission peaks of TAMRA and FAM (TAMRA/FAM ratios) generally decreased when water fractions in the microemulsion systems increased. This implies that a higher water content in the microemulsion systems resulted in less energy transfer or more distance between the fluorophores in the aqueous pseudo-phase of the microemulsion. Three parts of the resulting curve in Fig. 8 can be differentiated. At low water concentration (5–10%w/w, samples 2–3) TAMRA/FAM ratios were high and water was expected to be headgroup-bound in reverse micelles. When water concentrations were between 15 and 50%w/w (samples 3–11), TAMRA/FAM ratios steadily decreased, with an inflection point of the curve between 25–30%w/w of water (samples 6–7).

3. Discussion

Different techniques provided different data which supported and complemented each other to assist in the determination of the microstructures formed by IPP/water/Aerosol®OT: 1-butanol (2 : 1) microemulsions. Table 1 summarizes the findings.

The visual appearance of the samples indicated that samples 1–11 (0–50% w/w of water) are solutions or microemulsions since they were clear liquids with low viscosity. Sample 12 (55%w/w of water) might be liquid crystal be-

Table: Summary of results of various experimental techniques (critical changes) used to investigate the microstructure of IPP/water/Aerosol®OT: 1-butanol (2 : 1) microemulsions

Sample number	1	2	3	4	5	6	7	8	9	10	11	12
%w/w of water	0	5	10	15	20	25	30	35	40	45	50	55
Visual inspection	●	●	●	●	●	●	●	●	●	●	●	▼
PLM	●	●	●	●	●	●	●	●	●	●	●	▼
Cryo-FESEM	●	●	●	○	○	○	○	○	○	○	○	/
conductivity	●	●	●	◍	◍	◍	○	○	○	○	○	▼
viscosity	●	●	●	●	●	●	●	●	●	●	●	▼
DSC	●	●	●	●	○	○	○	○	○	○	○	▼
NMR (D of water)	/	●	●	◍	◍	◍	○	○	○	○	○	/
NMR (D of IPP)	●	●	●	●	○	○	○	○	○	○	○	/
FRET	/	●	●	◍	◍	◍	○	○	○	○	○	/

The different symbols indicate where a critical change in the data of the respective technique occurred. Symbols do not necessarily have the same meaning form technique to technique. Circles indicate a microemulsion, triangles indicate a liquid crystalline system and / = not determined

cause it was clear gel. The cross-polarized light microscopy confirmed that sample 12 was liquid crystal by showing birefringence. In the other samples, birefringence was not found.

Cryo-FESEM micrographs show that at low water concentration ($\leq$10%w/w), the system did not exhibit a discernable fine structure, and thus water might be headgroup bound to the surfactant molecules or very small reveres micelles may have formed. Globular structures could be found in samples containing 15–50%w/w of water which, in keeping with the appearance of droplet type microemulsions of other systems (Krauel et al. 2005), implied that they were droplet-type microemulsions. Interestingly, no bicontinuous structure was found. Furthermore, by using cryo-FESEM we could not clearly separate w/o and o/w droplet-type microemulsions in the systems investigated.

An increase in conductivity could be detected when the systems contained $\geq$10%w/w of water (sample 4); and a further increase in slope was found between 25–30%w/w of water (samples 6–7). These points therefore might represent transition points. Further dilution of over 50%w/w of water led to a decrease in conductivity coinciding with the formation of liquid crystals. When the systems contained 0–50%w/w of water, the viscosity was low and almost constant. Only the appearance of the liquid crystalline phase could be detected by viscosity.

The freezing of water could be observed in the DSC cooling curves when the systems contained >20%w/w of water (sample 5 onward) which implied that a transition might occur between 15–20%w/w of water. The NMR self-diffusion coefficient of water was higher than that of IPP when the systems contained $\geq$20%w/w of water (sample 5). A stronger increase in the water self-diffusion coefficient started at samples containing 30%w/w of water or more (samples 7–11). The NMR data thus suggested that two structural changes occur at around 15 and 30%w/w of water, respectively. The FRET experiment implies that reverse micelles were formed at low water concentration (5–10%w/w). The inflection point of the curve between 25–30%w/w (samples 6–7), is indicative of another transition (w/o to o/w microemulsion).

Comparing the experimental results, it can be concluded that a solution or reversed micellar system, w/o microemulsions, o/w microemulsions and liquid crystals formed in IPP/water/Aerosol®OT: 1-butanol (2 : 1) system depending on the water fraction. The transition from solution/reversed micelle to w/o microemulsion occurred between 10–15%w/w of water. The system then transformed to o/w microemulsion when it contained between 25–30%w/w of water and finally formed liquid crystal when water concentration was 55%w/w. The transitions however, appear to be gradual, as for example the DSC data indicates a transition between 15–20%w/w of water. The different types (w/o and o/w) of microemulsions characterised in this study will be used to incorporate with both hydrophobic and hydrophilic model drugs for investigation of skin permeation enhancement.

4. Experimental

4.1. Materials

Aerosol®OT (bis(2-ethylhexyl)sulfosuccinate sodium) was purchased from Fluka (Buchs, Switzerland). Isopropyl palmitate (IPP) was obtained from Uniquema (DE, USA). 1-Butanol was obtained from BDH Chemicals Ltd. (Poole, UK). 5(6)-FAM (5-(and-6)-carboxyfluorescein) and 5(6)-TAMRA (5-(and-6)-carboxytetramethyl-rhodamine) were purchased from Molecular Probes, Inc. (OR, USA). Distilled water was used throughout the experiments. All chemicals were used without further purification.

4.2. Construction of pseudoternary phase diagram

The pseudoternary phase diagram was constructed using the water titration method to find the concentration range of components for the existing range of IPP/water/Aerosol®OT: 1-butanol (2 : 1) microemulsions. Aerosol®OT and 1-butanol were mixed at the weight ratio of 2 : 1 to obtain the surfactant mixture. IPP and the surfactant mixture were mixed at the weight ratios of 1 : 9, 2 : 8, 3 : 7, 4 : 6, 5 : 5, 6 : 4, 7 : 3, 8 : 2 and 9 : 1. These mixtures were diluted dropwise with water under moderate agitation. Samples were identified as microemulsions when they appeared as clear liquids of low viscosity.

4.3. Preparation of samples

Aerosol®OT and 1-butanol were mixed in a 2 : 1 weight ratio to obtain the surfactant mixture. The concentration of the surfactant mixture was kept constant at 45%w/w while the concentration of water was varied from 0 to 55%w/w in 5%w/w intervals. The prepared samples represented a line in the pseudoternary phase diagram (Fig. 1). The required amounts of surfactant mixture, IPP and water were mixed using a vortex mixer for 5 min at room temperature. All samples were stored at room temperature for at least 24 h to equilibrate before further characterisation.

4.4. Appearance observation

The samples were observed for visual and microscopic appearance. A cross-polarized light microscope (Nikon Optiphot PFX microscope, Tokyo, Japan) was used.

4.5. Cryo-Field Emission Scanning Electron Microscopy (Cryo-FESEM)

Samples were loaded into copper rivets and plunge frozen in liquid propane with a Reichert KF 80 (Leica, Germany). Samples were then transferred under liquid nitrogen to an Alto 2500 cryo preparation chamber (Gatan, UK), fractured and transferred onto the cryo-stage of a JEOL 6700F field emission scanning electron microscope (JEOL, Japan). Samples were etched at $-95\,^{\circ}C$ for approximately 4 min and then transferred back into the cryo chamber for sputter coating with platinum. Samples were then introduced back onto the cryo stage of the microscope and viewed at an accelerating voltage of 2.5 kV.

4.6. Conductivity measurements

Electrical conductivity of the samples was measured using a Riac CM/100 conductivity meter fitted with an YSI 3418 electrode (Yellow Springs Instruments Inc., OH, USA). The cell constant was 0.11 cm^{-1}. The measurements were carried out in triplicate at 25 °C.

4.7. Viscosity measurements

Viscosity of the samples was measured using a Brookfield DV-III programmable cone and plate rheometer (Brookfield Engineering Laboratories Inc., MA, USA) fitted with a CP-42 cone spindle. Brookfield Rheocalc operating software controlled the rheometer. The jacketed sample cup was connected to a circulating water bath operating at 25 °C. A sample volume of 1 ml was used. The measurements were carried out in triplicate at 25 °C.

4.8. Differential Scanning Calorimetry (DSC)

DSC measurements were performed with a differential scanning calorimeter TA Q100 equipped with a refrigerated cooling system (TA Instruments, DE, USA). Nitrogen with a flow of 50 ml/min was used as purge gas. Approximately 4–13 mg of sample was weighted precisely into a hermetic aluminum pan and then sealed. An empty sealed pan was used as a reference. Samples were cooled from 25 to $-50\,^{\circ}C$ at a cooling rate of 5 °C/min. All measurements were performed in triplicate. Freezing temperatures were recorded as peak onsets.

4.9. Nuclear Magnetic Resonance Spectroscopy (NMR)

Self-diffusion NMR measurements were performed on a Varian Inova (500 MHz) equipped with Performa II-Z gradient coils. The temperature was kept constant at 25 °C. Each sample was filled into a 3 mm diameter NMR tube (Wilmad-Labglass, Buena, NJ, USA). 2,2-Dimethyl-2-silapentane-5-sulfonate sodium salt (DSS) dissolved in D_2O and sealed into a capillary was used as reference. ^1H NMR spectra of the pure components were taken and compared with those of the microemulsions to obtain a characteristic peak shift for water and IPP for the later analysis. Experiments were performed by keeping the z-gradient pulse length constant and gradually increasing the gradient strength in 17 steps. The gradient pulse length used was 100 ms to measure the diffusion coefficient of all components. The diffusion coefficients (D) were obtained from the slope of Eq. (1):

$$\ln(I_g/I_0) = -[\gamma^2 d^2 G^2 (\Delta - d/3)]\, D \qquad (1)$$

where I_g and I_0 are intensities of the NMR signal in the presence and absence of field gradient pulses, γ is the gyromagnetic constant for ^1H, d is the duration of the z-gradient pulse, G is the gradient strength and Δ is the time interval between the gradient pulses.

4.10. Fluorescence resonance energy transfer (FRET)

In order to investigate the microemulsion samples by FRET, a solution of mixed fluorescence dyes (0.01 μg/ml of 5(6)-FAM and 0.1 μg/ml of 5(6)-TAMRA) in distilled water was used as aqueous phase in sample preparation. The emission spectra of the dye solutions and the samples were measured with a spectrofluorometer (RF 540, Shimadzu Corporation, Kyoto, Japan) using an excitation wavelength of 488 nm, at which the absorption spectrum of the acceptor (5(6)-TAMRA) overlapped with the fluorescence emission spectrum of the donor (5(6)-FAM). The ratio of the emission intensity maximum of the 5(6)-TAMRA peak (570 nm) and the emission intensity maximum of the 5(6)-FAM peak (515 nm) was calculated for each sample.

Acknowledgements: The authors are grateful for financial support received from the Thailand Research Fund through the Royal Golden Jubilee Ph.D. Program (PHD/0146/2544). Mervyn Thomas, Liz Girvan and Kevin Crump are thanked for technical assistance.

References

Alany RG, Rades T, Agatonovic-Kustrin S, Davies NM, Tucker IG (2000) Effects of alcohols and diols on the phase behaviour of quaternary systems. Int J Pharm 196: 141–145.

Alany RG, Tucker IG, Davies NM, Rades T (2001) Characterizing colloidal structures of pseudoternary phase diagrams formed by oil/water/amphiphile systems. Drug Dev Ind Pharm 27: 31–38.

Bumajdad A, Eastoe J (2004) Conductivity of water-in-oil microemulsions stabilized by mixed surfactants. J Colloid Interface Sci 274: 268–276.

Changez M, Varshney M (2000) Aerosol-OT microemulsions as transdermal carriers of tetracaine hydrochloride. Drug Dev Ind Pharm 26: 507–512.

El-Laithy HM (2003) Preparation and physicochemical characterization of dioctyl sodium sulfosuccinate (Aerosol OT) microemulsion for oral drug delivery. AAPS Pharm Sci Tech 4: Article 11.

Friberg SE (1990) Micelles, microemulsions, liquid crystals, and the structure of stratum corneum lipids. J Soc Cosmet Chem 41: 155–171.

Garti N, Aserin A, Tiunova I, Fanun M (2000) A DSC study of water behavior in water-in-oil microemulsions stabilized by sucrose esters and butanol. Colloids and Surfaces A: Physicochem Eng Aspects 170: 1–18.

Gupta RR, Jain SK, Varshney M (2005) AOT water-in-oil microemulsions as a penetration enhancer in transdermal drug delivery of 5-fluorouracil. Colloids and Surfaces B: Biointerfaces 41: 25–32.

Ko CJ, Ko YJ, Kim DM, Park HJ (2003) Solution properties and PGSE-NMR self-diffusion study of $C_{18:1}E_{10}$/oil/water system. Colloids and Surfaces A: Physicochem Eng Aspects 216: 55–63.

Krauel K, Davies NM, Hook S, Rades T (2005) Using different structure types of microemulsions for the preparation of poly(alkylcyanoacrylate) nanoparticles by interfacial polymerization. J Control Rel 106: 76–87.

Kreilgaard M, Pedersen EJ, Jaroszewski JW (2000) NMR characterisation and transdermal drug delivery potential of microemulsion systems. J Control Rel 69: 421–433.

Lawrence MJ, Rees GD (2000) Microemulsion-based media as novel drug delivery systems. Adv Drug Deliv Rev 45: 89–121.

Lovullo D, Daniel D, Yodh J, Lohr D, Woodbury NW (2005) A fluorescence resonance energy transfer-based probe to monitor nucleosome structure. Analytical Biochem 341: 165–172.

Mitra RK, Paul BK (2005) Physicochemical investigations of microemulsification of eucalyptus oil and water using mixed surfactants (AOT + Brij-35) and butanol. J Colloid Interface Sci 283: 565–577.

Moshe MB, Magdassi S, Cohen Y, Avram L (2004) Structure of microemulsions with gemini surfactant studied by solvatochromic probe and diffusion NMR. J Colloid Interface Sci 276: 221–226.

Moulik SP, Paul BK (1998) Structure, dynamics and transport properties of microemulsions. Adv Colloid Interface Sci 78: 99–195.

Paul BK, Moulik SP (1997) Microemulsions: an overview. J Dispersion Sci Tech 18(4): 301–367.

Podlogar F, Gašperlin M, Tomšič M, Jamnik A, Rogac MB (2004) Structural characterisation of water-Tween 40®/Imwitor 308®-isopropyl myristate microemulsions using different experimental methods. Int J Pharm 276: 115–128.

Selvin PR (2000) The renaissance of fluorescence resonance energy transfer. Nature Struct Biol 7: 730–734.

Stilbs P (1987) Fourier transform pulsed-gradient spin-echo studies of molecular diffusion. Progress in NMR Spectroscopy 19: 1–45.

Takenaka S, Ueyama H, Nojima T, Takagi M (2003) Comparison of potassium ion preference of potassium-sensing oligonucleotides, PSO-1 and PSO-2, carrying the human and oxytrica telomeric sequence, respectively. Anal Bioanal Chem 375: 1006–1010.